PAPER

Check for updates

Theoretical investigations on azole-fused tricyclic 1,2,3,4-tetrazine-2-oxides†

Teng Fei, [ID] Yao Du, [ID] Chunlin He* and Siping Pang [ID] *

Fused compounds, a unique class of large conjugate structures, have emerged as prime candidates over traditional nitrogen-rich mono-ring or poly-ring materials. Meanwhile, compounds containing catenated nitrogen chains have also attracted attention from scientists due to their high heats of formation. On the other hand, the azoxy [−N═N(O)−] moiety has been found to increase density effectively in the molecular structure of compounds. Therefore, combining fused heterocyclic organic skeletons with the azoxy moiety can be regarded as an effective method for increasing the density and heat of formation, which results in substantial increase in detonation properties. Based on the above-mentioned considerations, in this study, a series of new non-hydrogen-containing 5/6/5 fused ring molecules with azoxy moiety structures are designed. Furthermore, their properties as potential high-energy-density materials, including their density, heats of formation, detonation properties, and impact sensitivity, have been extensively evaluated using thermodynamic calculations and density functional theory. Among the investigated compounds, 1,3,8,10-tetranitrodiimidazo[1,5-*d*:5′,1′-*f*][1,2,3,4]tetrazine 5-oxide (**B**), 1,10-dinitrobis([1,2,3]triazolo)[1,5-*d*:5′,1′-*f*][1,2,3,4]tetrazine 5-oxide (**C**) and 2,9-dinitrobis([1,2,4]triazolo)[1,5-*d*:5′,1′-*f*][1,2,3,4]tetrazine 5-oxide (**D**) display remarkable stabilities and are predicted to be high-performance energetic materials due to their high density (>1.94 g cm^{-3}), detonation velocity (>9616 m s^{-1}), and detonation pressure (>41.1 GPa). In addition, our design strategy, which combines the azoxy moiety and fused tricyclic skeleton to construct nitrogen-rich molecular structures with high density and positive heat of formation, is a valuable approach for developing novel high-energy-density materials with excellent performance and stability.
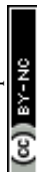
Introduction

In the pursuit of high-performance energetic materials, nitrogen-rich five- or six-membered heterocycles possessing high densities, high heats of formation, and good oxygen balance are widely sought.[1–4] Among these newly emerging structural motifs, the family of fused polycyclic azoles and azines is attracting increasing interests, and these materials have been utilized for designing various highly energetic nitrogen-rich skeletons. Recently, various remarkable novel fused heterocyclic compounds, for example, tetrazino-tetrazine 1,3,6,8-tetraoxide (TTTO),[5] 4-amino-3,7-dinitro-triazolo-[5,1-*c*][1,2,4] triazine-4-oxide (DPX-27),[6] and 3,6,7-tri-amino-[1,2,4]triazolo[4,3-*b*][1,2,4]triazole (TATOT)[7] have been reported. Due to their high nitrogen content and planar structure, these energetic molecules exhibit a good balance between high performance and low sensitivity. Significantly, non-hydrogen-containing 5/6/5 fused ring energetic

compounds such as 1,2,9,10-tetranitrodipyrazolo[1,5-*d*:5′,1′-*f*][1,2,3,4]-tetrazine[8] and 2,9-dinitrobis([1,2,4]triazolo)[1,5-*d*:5′,1′-*f*][1,2,3,4]tetrazine[9] have received considerable attention due to their special molecular structures. In their molecular organization, two dinitropyrazole or dinitrotriazole rings are fused to 1,2,3,4-tetrazine with six concomitant catenated nitrogen atoms. These molecules exhibit clear advantages of thermal stability and excellent energetic performance. Therefore, fused nitrogen-rich heterocycles have been identified as a promising family of organic skeletons for energetic materials.

Furthermore, nitrogen-rich heterocycles have become the core motif in the search for new HEDMs, and their compatibility with other energetic functionalized groups is receiving increasing attention.[10] During the past decade, several studies have been reported on the potential beneficial energetic properties of the azo group.[11–13] The presence of the azo in energetic compounds allows for higher detonation velocities, pressures and densities in azo compounds, as determined by experimental measurements and theoretical calculations. However, the search for new energetic compounds with better properties is ongoing. In addition to introducing the azo group, the introduction of N-oxides is a rather recent methodology. The

School of Materials Science & Engineering, Beijing Institute of Technology, Beijing 100081, P. R. China. E-mail: chunlinhe@bit.edu.cn; pangsp@bit.edu.cn
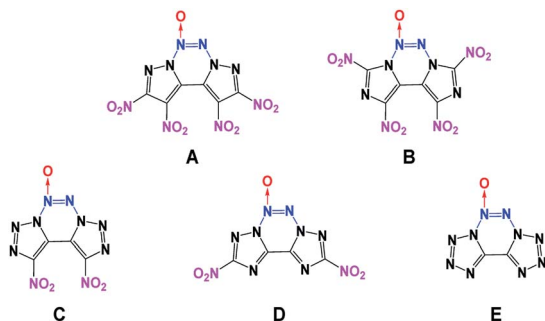
Fig. 1 The designed novel azoxy-fused tricyclic compounds in this study.

additional oxygen atom coordinated to the nitrogen system not only enhances density and performance but also tends to stabilize the entire molecule;[14–16] for example, 4,4′- bis(nitramino)azofurazan has density of 1.89 g cm^{-3}, detonation velocity of 9517 m s^{-1}, and detonation pressure of 41.1 GPa.[17] After the formation of the azoxy compound 4,4′-bis(nitramino)-azoxyfurazan,[17] its density and energetic properties are further enhanced; it exhibits density of 1.96 g cm^{-3}, detonation velocity of 9746 m s^{-1}, and detonation pressure of 44.1 GPa. On the basis of the experimental measurements and theoretical calculations, the higher values for detonation velocities and pressures and higher densities for azoxy compounds support the advantages of the presence of an N-oxide moiety in energetic materials.

Generally, high density and positive heat of formation result in higher performance.[18] Therefore, combining fused heterocyclic organic skeletons with the azoxy moiety can be regarded as an effective method for increasing density and heat of formation. However, among the N-oxide energetic compounds, molecules that contain the azoxy [–N═N(O)–] moiety are hardly reported.[17,19] To the best of our knowledge, fused heterocyclic energetic compounds containing an azoxy moiety are rare and particularly, there are no known non-hydrogen-containing 5/6/5 fused tricyclic compounds with the azoxy moiety. Therefore, in this study, five new energetic molecules with fused tricyclic heterocyclic structures containing the azoxy moiety have been designed (Fig. 1). Before their synthesis, it is necessary to predict their performance in advance for security reasons. Fortunately, modern theoretical studies based on quantum chemical treatments have gained acceptance as a useful research tool for screening candidate high-energy-density materials (HEDMs), thereby avoiding expensive and dangerous experimental tests. Such studies can provide an understanding of the relationships between molecular structures and properties, which can then be used to design better and more efficient laboratory tests. The present theoretical investigation may further help the experimental synthesis and testing of these novel energetic compounds.

Computational methods

Theoretical calculations were performed using the Gaussian 09 series of programs.[20] The geometric optimization and frequency

analyses were completed using the B3LYP functional combined with the 6-311++G** basis set. The single energy points were calculated at the MP2/6-311++G** level of theory. Harmonic vibrational frequencies including IR spectra and thermochemical parameters were obtained at the same levels of theory. Meanwhile, the electronic properties, highest occupied molecular orbital (HOMO), lowest unoccupied molecular orbital (LUMO), and electrostatic potential on the molecular surface of the title compounds were calculated at the B3LYP/6-311++G** level of theory based on their optimized gas-phase structures. For all the compounds, their optimized structures were characterized as true local energy minima on the potential energy surface without imaginary frequencies. The final task was to establish the solid-state heat of formation ($\Delta H_{f,solid}$) for all the synthesized compounds. $\Delta H_{f,solid}$ of neutral compounds can be estimated by subtracting the heat of sublimation (ΔH_{sub}) from the gas-phase heat of formation ($\Delta H_{f,gas}$). According to Hess's law of constant heat summation,[21] $\Delta H_{f,gas}$ and ΔH_{sub} can be used to evaluate $\Delta H_{f,solid}$ as follows:

$$\Delta H_{f,solid} = \Delta H_{f,gas} - \Delta H_{sub} \qquad (1)$$

According to Politzer et al.,[22,23] ΔH_{sub} can be computed from the corresponding molecular surface area and electrostatic interaction index $\nu\sigma_{tot}^2$ for energetic compounds. The empirical expression of this approach is

$$\Delta H_{sub} = aA^2 + b(\nu\sigma_{tot}^2)^{0.5} + c \qquad (2)$$

where A is the surface area of the 0.001 electrons per bohr^3 isosurface of the electronic density of the molecule, ν describes the degree of balance between the positive and negative potential on the isosurface, and $\nu\sigma_{tot}^2$ is a measure of the variability of the electrostatic potential on the molecular surface. The coefficients a, b, and c were determined by Rice et al.:[24] $a = 2.670 \times 10^{-4}$ kcal mol^{-1} Å^{-4}, $b = 1.650$ kcal mol^{-1}, and $c = 2.966$ kcal mol^{-1}. This approach has been used to credibly evaluate the heats of sublimation of many energetic compounds.[25,26] In this study, the surface area, degree of balance between the positive and negative surface potentials and variability of the electrostatic potential were calculated using the Multiwfn program.[27]

For each neutral compound, the theoretical density was initially determined from the molecular weight (M) divided by V_m, where V_m is the van der Waals volume, which was obtained by Monte Carlo integration using the Multiwfn program. By introducing the interaction index $\nu\sigma_{tot}^2$, the density of an energetic compound can be corrected according to the following equation, where $\alpha = 1.0462$, $\beta = 0.0021$, and $\gamma = -0.1586$.

$$\rho = \alpha \frac{M}{V} + \beta(\nu\sigma_{tot}^2) + \gamma \qquad (3)$$

The calculations of the detonation parameters such as detonation velocity (D), detonation pressure (P), heat of detonation (Q) and explosion temperature (T_{det}) were performed with the EXPLO5 program package (version 6.01).[28]

The bond dissociation energy (BDE) can provide useful information for understanding the stability of a molecule. Generally, the smaller the energy for breaking a bond, the weaker the bond, making it easier for the bond to act as a trigger bond. For many organic molecules, the terms "bond dissociation energy" (BDE) and "bond dissociation enthalpy" often appear interchangeably in the literature.[29]

At 0 K, BDE is given as:

$$BDE_0(A\text{--}B) \rightarrow E_0(A^{\cdot}) + E_0(B^{\cdot}) - E_0(A\text{--}B) \qquad (4)$$

BDE with a ZPE correction can be calculated using the following equation:

$$BDE(A\text{--}B)_{ZPE} \rightarrow BDE_0(A\text{--}B) + \Delta E_{ZPE} \qquad (5)$$

here, ΔE_{ZPE} is the difference between ZPEs of the products and the reactants.

Mulliken atomic charge analysis of nitro groups is also used to estimate the impact sensitivities of the title compounds. Normally, for the majority of nitro explosives, the R–NO$_2$ (R = N, C or O) bonds are the weakest bonds and their breaking is usually the initial step in decomposition or detonation. The nitro group charge ($-Q_{NO_2}$) is calculated by the sum of the net Mulliken atomic charges on the nitrogen and oxygen atoms of the nitro group:

$$-Q_{NO_2} = Q_N + Q_{O(1)} + Q_{O(2)} \qquad (6)$$

To investigate the sensitivity of the title compounds, the property–structure relation method, i.e., "generalized interaction property function" was used to estimate the impact sensitivity, $h_{50\%}$. Here, we give four introduced methods, as summarized below:[30,31]

Method 1: $h_{50\%} = 9.2 + 8.04 \times 10^2 \times \exp$
$$[-(0.0875 \text{ mol kJ}^{-1} \times |\bar{V}^+ - |\bar{V}^-\|)] \qquad (7)$$

Method 2: $h_{50\%} = 29.3 + 1.386 \times 10^{-3} \times \exp[48.84v] \qquad (8)$

Method 3: $h_{50\%} = 27.8 + 0.1135 \times \exp$
$$[-(2.6479 \text{ g kJ}^{-1} \times [Q_d - 6.9496 \text{ kJ g}^{-1}])] \qquad (9)$$

Method 4: $h_{50\%} = 1.341 \times \exp$
$$[8.1389v - 1.6234 \text{ g kJ}^{-1} \times (Q_d - 6.166) \text{ kJ g}^{-1}] \qquad (10)$$

here, $|\bar{V}^+ - |\bar{V}^-\||$ is the difference between the magnitudes of the averages of the positive and negative values of the electrostatic potential, v is the balance parameter, and Q_d is the heat of detonation. To compare with the impact energy when 2.5 kg hammer is used, $h_{50\%}$ of 100 cm is equivalent to the impact energy of 24.5 J.[32]

The electric spark sensitivity shows the degree of sensitivity of an explosive to an electric discharge. The electric spark sensitivity of the title compounds is calculated using the following equation:[33]

$$E_{ES} \text{ (J)} = (-1)^{n_1} 10.16 Q_{NO_2} - 1.05 n_1 n_2 E_{LUMO} - 0.20 \qquad (11)$$

here, n_1 is the number of aromatic rings, n_2 is the number of substituted groups attached to the aromatic ring, Q_{NO_2} is the minimum Milliken charge of the nitro group and E_{LUMO} (in eV) is the lowest unoccupied molecular orbital energy.

Results and discussion

Structural design and molecular geometry

For energetic materials, the pursuit of higher energy is a constant goal. Recently, a tricyclic skeleton structure, that is, a non-hydrogen-containing 5/6/5 fused tricyclic structure was reported, in which two five-membered azole heterocycles and a 1,2,3,4-tetrazine are combined via a common C–N bond. From the view of structural design of new energetic compounds, this tricyclic compound offers a potentially promising skeleton for the construction of novel C-nitro-based energetic materials through different nitration reactions. The advantages of this tricyclic skeleton are as follows: (1) the tricyclic structure can provide additional ring strain, thereby making active contribution to the high positive $\Delta H_{f,solid}$ of energetic materials; (2) the replacement of the hydrogen atoms with nitro groups in azole heterocycles can greatly increase their oxygen balance (OB) and therefore improve the detonation performance of the resulting compounds. On the other hand, from the viewpoint of molecular design, energetic compounds with high densities (ideally higher than 2.0 g cm^{-3}) are particularly desirable since the detonation pressure and velocity of explosives are directly related to their density (ρ). If ρ can be further enhanced on the basis of this structure, the energetic properties can be further improved. According to calculations and experiments, the presence of an azoxy group in energetic compounds allows for higher D, P and ρ. Therefore, combining the non-hydrogen-containing 5/6/5 fused tricyclic structure with the azoxy moiety can achieve a satisfactory result in theory.

In the first design strategy, pyrazole, imidazole, 1,2,3-triazole, 1,2,4-triazole and tetrazole were chosen as potential initial structures for combination with 1,2,3,4-tetrazine via common C–C and C–N bonds, and this resulted in the formation of novel skeletons with fused tricyclic structures. These compounds contained at least six nitrogen atoms with the goal of ensuring a high positive $\Delta H_{f,solid}$ value for the resultant molecules. In the second phase, –N=N(O)– was replaced with the –N=N– moiety to form new energetic molecules, which have higher ρ and OB. Considering that the pyrazole, imidazole, 1,2,3-triazole and 1,2,4-triazole moieties have two or four positions that can be further modified, several energetic groups, such as nitroamine and azide functional groups, can be introduced with the goal of ensuring that the resultant new molecules have high energy densities.

Among them, the nitro group is considered to be one of the superior explosophores because of the favorable balance between stability and performance. In comparison, the nitroamino and azido functionalities tend to increase density and detonation properties; however, their molecular stabilities associated with thermal behavior and impact and friction sensitivity are not competitive with those of their nitro-
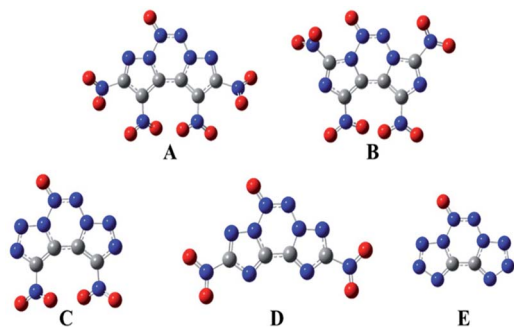
Fig. 2 Molecular structures of the designed compounds.

functionalized analogues.[34] Therefore, in the third phase, to further enhance the energy level, two or four nitro groups were introduced *via* C-functionalization. All the designed target compounds have N10 structures (contain 10 nitrogen atoms). Additionally, compounds **C** and **E** have 8 and 10 catenated nitrogen atoms in their structures, respectively.

The geometric structures of all the compounds were optimized based on the true local energy minima on the potential energy surface without imaginary frequencies. To help understand the geometric constructions, the optimized structures of **A–E** are shown in Fig. 2. The surface analyses of **A–E** are summarized in the ESI.† From Fig. 2, it can be seen that compound **D** remained coplanar after substitution with nitro groups. However, after nitration of the precursor compounds of **A–C**, the nitro group and the ring formed a dihedral angle in the range of 35–85°, which may improve their crystal packing. The three heterocycles in the fused tricyclic system and N→O bond were co-planar, whereas the nitro groups deviated from the ring plane, implying that their electronic properties play an important role in their molecular structure.

Electrostatic potentials and frontier molecular orbital energies

The electrostatic potential (ESP) on a molecular surface can help understand its intermolecular interaction and can also help predict its chemically reactive sites.[35] The ESP mapped van der Waals surfaces of compounds **A–E** are shown in Fig. 3. Only the global minima and maxima on their surfaces are labelled in bold font. The surface areas in each ESP range are plotted in the ESI.† It can be seen that in the **A–E** unit region, the surface minima of ESP are observed between the oxygen atoms, especially the oxygen atoms of the nitro group bonded to the carbon atom, because of their higher electronegativity, and these are the primary electrophilic sites. The global maxima of ESP on the **A–E** surfaces range from +63.85 to +69.58 kcal mol^{-1}, corresponding to 1,2,3,4-tetrazine, whereas minima from −18.32 to −21.79 kcal mol^{-1} correspond to the oxygen atoms of the nitro group. The strongly positive ESP surface (red) is prominent in the center of the molecule, whereas the negative ESP surface (blue) primarily caused by electron-withdrawing groups (–NO$_2$) is in the surrounding of the molecule. These observations are consistent with the atomic charges obtained from the subsequently mentioned natural bond orbital analysis.

The highest occupied molecular orbitals (HOMOs) and the lowest unoccupied molecular orbitals (LUMOs) are named as frontier molecular orbitals (FMOs). The energy gap between the HOMO and the LUMO (ΔE) is an important parameter to evaluate molecular stability, especially for compounds with similar skeletons.[36,37] A small ΔE value can lead to enhanced reactivity and poor stability with respect to chemical and photochemical processes.[38] For example, it causes electrons to transition from the HOMO to LUMO easily, thus leading to the molecule becoming less stable. The HOMOs and LUMOs including the energy gap are depicted in Fig. 4. The red color represents the positive phase, and the green color represents the negative phase. As can be seen from Fig. 4, the HOMOs of all the
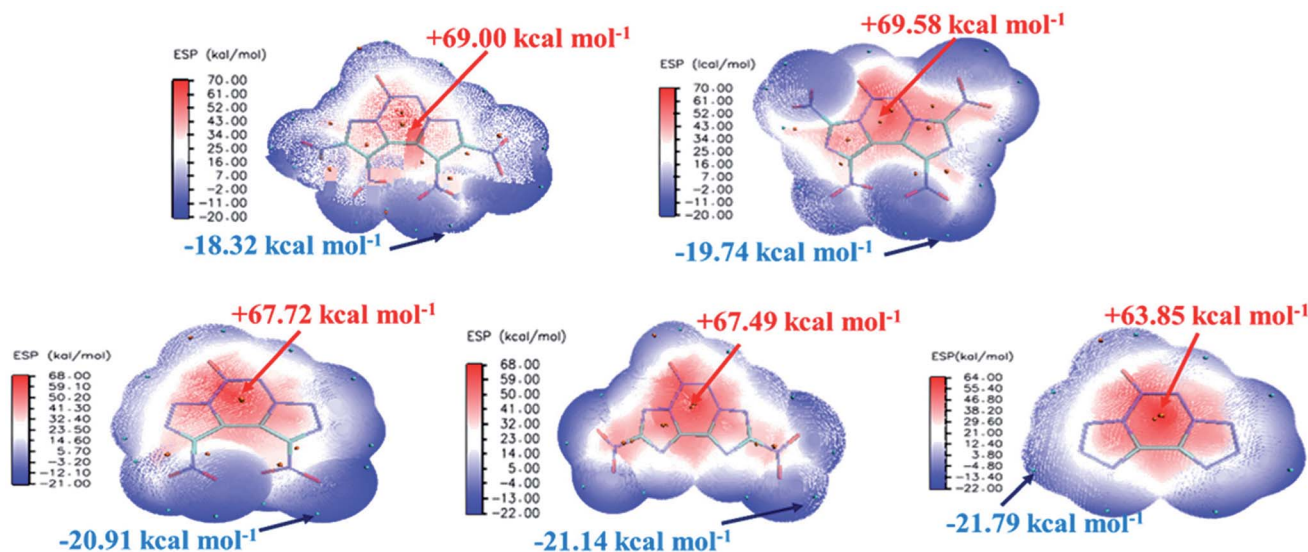

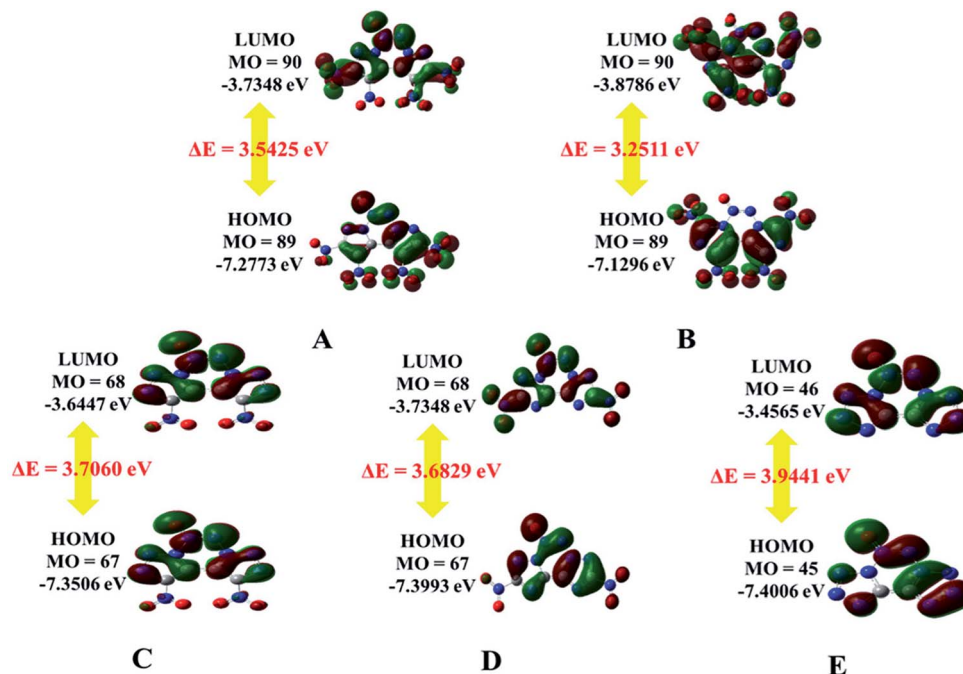Fig. 3 ESP mapped molecular van der Waals surface of compounds A−E.

Fig. 4 HOMO and LUMO orbitals of **A–E**.

molecules are localized approximately on the fused tricyclic structure. In addition, ΔE of **E** (3.9441 eV) is the largest and that of **B** (3.2511 eV) is the smallest, indicating that the former is more stable than the latter. All the compounds are complete nitrification products (except for **E**), which indicates that the more nitro groups they possess, the less stable they are. Again, the magnitudes imply that the predicted sequence of stability is **B** < **A** < **D** < **C** < **E**, and the order is reversed for the chemical activity of the title compounds.

Natural bond orbital charges and electronic density

Natural bond orbital charges (NBO) can provide useful information on the distribution of charges and other chemical properties. Generally, high peaks correspond to the nuclear

charge of a heavy nucleus, which improves electron aggregation and displays integral exponential attenuation towards all surrounding atoms.[39] The Multiwfn program was used to calculate density, and the contour line maps of the electronic density on **A–E** are shown in Fig. 5. The electron densities around oxygen and nitrogen atoms are higher than those around other atoms due to their strong electronegativity. Generally, electrons prefer to assemble in the bonding area (such as A1, B1, C1, D1 and E1) because of electron pair sharing between atoms bonded covalently. The electron densities around the oxygen and nitrogen atoms are higher than those around other atoms due to strong electronegativity; the electron densities around O13 are higher than those around other atoms (A2, B2, C2, D2 and E2). Moreover, delocalization also occurs in
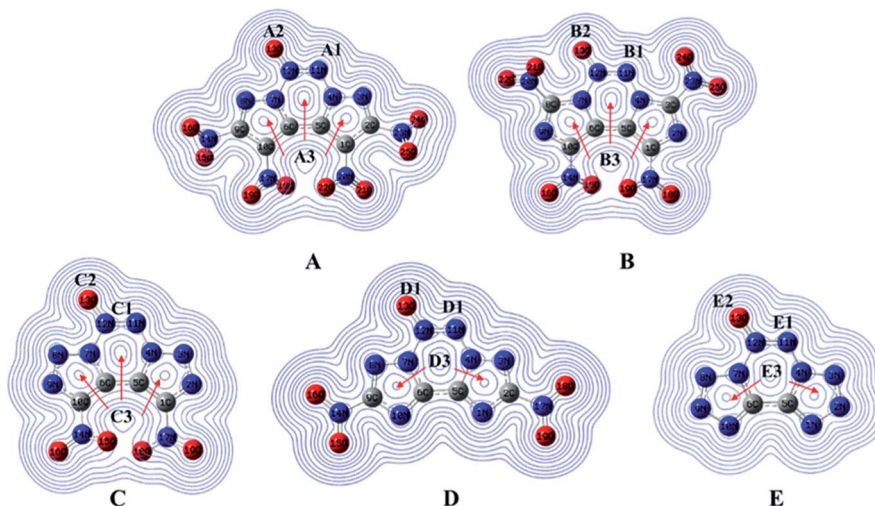

Fig. 5 Electronic density and charges of the designed molecules.

Table 1   NBO charges for the atoms in compounds A–E

A		B		C		D		E	
Atom	Charge	Atom	Charge	Atom	Charge	Atom	Charge	Atom	Charge
1C	0.03844	1C	0.28245	1C	0.24662	1N	−0.40933	1N	−0.24324
2C	0.29824	2N	−0.38239	2N	−0.18982	2C	0.45835	2N	−0.02998
3N	−0.20285	3C	0.50248	3N	−0.00817	3C	−0.21354	3N	−0.02525
4N	−0.00205	4N	−0.20611	4N	−0.02386	4C	−0.02407	4N	−0.05047
5C	0.14488	5C	0.11291	5C	0.09983	5N	0.31421	5C	0.28917
6C	0.15709	6C	0.14506	6C	0.14005	6C	0.36744	6C	0.32211
7N	−0.04202	7N	−0.25574	7N	−0.06589	7N	−0.06832	7N	−0.08171
8N	−0.19494	8C	0.51418	8N	0.00147	8N	−0.2087	8N	−0.01435
9C	0.30618	9N	−0.37411	9N	−0.17363	9C	0.47063	9N	−0.01277
10C	0.04704	10C	0.27497	10C	0.2432	10N	−0.41328	10N	−0.24403
11N	−0.03583	11N	−0.02563	11N	−0.03352	11N	−0.04001	11N	−0.03935
12N	0.44867	12N	0.45913	12N	0.45146	12N	0.44692	12N	0.44751
13O	−0.30751	13O	−0.32551	13O	−0.30624	13O	−0.31165	13O	−0.31763
14N	0.48666	14N	0.48966	14N	0.48942	14N	0.47294	—	—
15O	−0.33272	15O	−0.36947	15O	−0.35975	15O	−0.3218	—	—
16O	−0.30991	16O	−0.31006	16O	−0.31203	16O	−0.32883	—	—
17N	0.50622	17N	0.48938	17N	0.48809	17N	0.47248	—	—
18O	−0.35162	18O	−0.30994	18O	−0.37328	18O	−0.33522	—	—
19O	−0.31271	19O	−0.37635	19O	−0.31393	19O	−0.3282	—	—
20N	0.50409	20N	0.47744	—	—	—	—	—	—
21O	−0.31787	21O	−0.32654	—	—	—	—	—	—
22O	−0.36784	22O	−0.30204	—	—	—	—	—	—
23N	0.48726	23N	0.47074	—	—	—	—	—	—
24O	−0.31447	24O	−0.34369	—	—	—	—	—	—
25O	−0.33242	25O	−0.31082	—	—	—	—	—	—

the fused tricyclic structure, marked as A3 to E3, which may improve the stability of the ring skeleton as well as the molecular structure. To fully investigate the interactions among bonds, their NBO charges[40] are summarized in Table 1. Clearly, atom O13 is the most negative since N→O is a strong electron-withdrawing group. The nitro group accommodates higher positive charges because of its strong electronegativity and thus, it attracts electrons towards itself.

Infrared spectra

Infrared spectrum (IR) is useful to identify the functional groups of substances. The simulated infrared spectra of A–E are shown in Fig. 6; the horizontal axis represents frequency, and the vertical axis denotes intensity. The frequency value obtained from the DFT calculations is scaled down by a factor of 0.9668.[41] The calculated IR results show that the most intense IR peaks are observed at 1561, 1552, 1558, 1550 and 1546 cm^{-1} for compounds A–E, respectively, which correspond to the stretching vibration of their N→O bonds. The symmetric and asymmetric stretching vibrations of the N–O bond in the nitro groups of compounds A–D vary in the range from 1522 to 1570 cm^{-1}, and these values are very close to those of the stretching vibrations of the N→O bond. Meanwhile, the peaks at 845, 844, 818 and 815 cm^{-1} correspond to the vibrations of torsion for the nitro group in compounds A–D. The medium intense peaks in the range from 1000 to 1300 cm^{-1} are mainly due to the stretching vibrations of C–N and N–N bonds in the fused tricyclic skeleton. For compound E, the weak peaks near

826 cm^{-1} are mainly ascribed to the asymmetric stretching vibration of the tetrazole backbone.

Heat of formation

$\Delta H_{f,solid}$ is an important property for predicting the detonation properties of energetic materials. Therefore, to estimate D and P of an explosive molecule through theoretical calculations, the $\Delta H_{f,solid}$ value must be obtained. To obtain more accurate calculation results, the basic ring skeleton of the parent compound was kept invariable during the designed isodesmic reactions. The designed isodesmic reactions used to obtain $\Delta H_{f,gas}$ for the investigated compounds are shown in Scheme 1.

Table 2 lists the total energies (E_0), ZPEs, thermal corrections (H_T), and $\Delta H_{f,gas}$ for the reference compounds in the isodesmic reactions. The $\Delta H_{f,gas}$ value of each compound was calculated from the atomization reaction at the G2 level. Table 3 summarizes the calculated $\Delta H_{f,solid}$ values and the parameters related to $\Delta H_{f,solid}$ of all the designed compounds. It has been found that all the title compounds have positive $\Delta H_{f,solid}$ values over 580 kJ mol^{-1} due to a large number of inherently energetic CN and NN bonds in their structures. Among them, compound E has the largest $\Delta H_{f,solid}$ of 1092.8 kJ mol^{-1} due to the ten-nitrogen catenated chain in its structure. Besides, upon comparing these compounds, $\Delta H_{f,solid}$ can be summarized as follows: B < A < D < C < E, which indicates that $\Delta H_{f,solid}$ is strongly influenced by the length of the nitrogen chains and slightly affected by the number of nitro groups. It is worth noting that the introduction of the azoxy moiety leads to a decrease in $\Delta H_{f,solid}$ of this non-hydrogen-containing 5/6/5
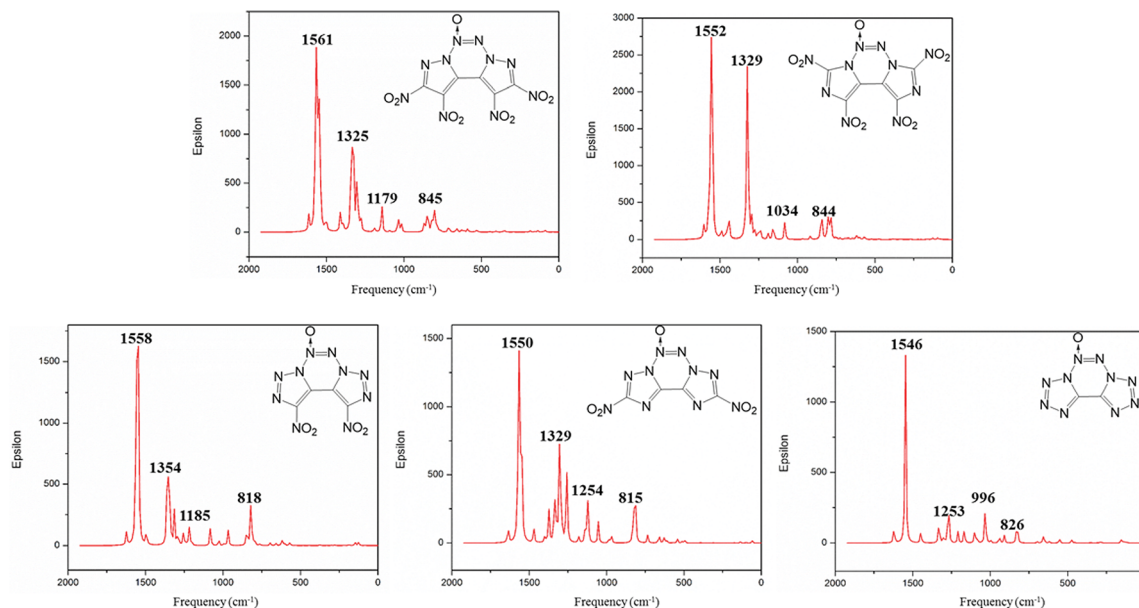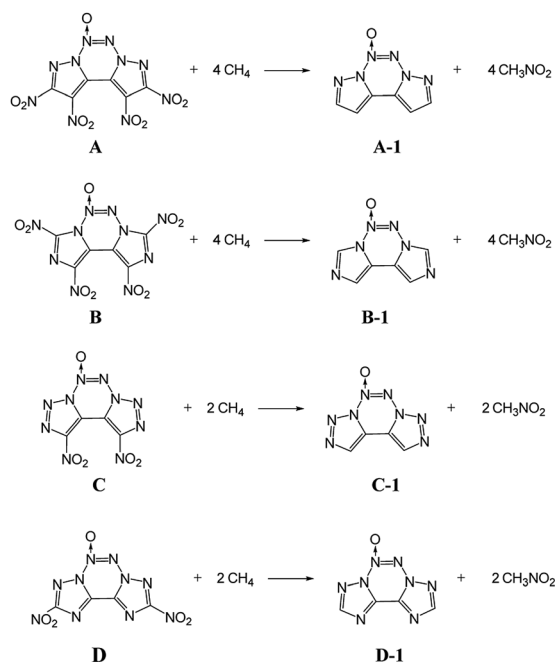
Fig. 6 Calculated IR spectra of compounds A–E.

fused tricyclic structure. Clearly, compounds **A** and **E** have the $\Delta H_{f,solid}$ values of 678.06 and 753.81 kJ mol^{-1}, which are reduced to 80 and 34 kJ mol^{-1}, respectively, compared to their non-azoxy structures.[8,9]

Thermodynamic properties are important for explosives; they are used to describe a chemical system that neither consumes nor releases heat energy and to predict thermal stability in a chemical reaction. On the basis of vibrational analysis and the statistic thermodynamic method, the thermodynamic functions such as thermal correction to internal energy (U), enthalpy (H), free energy (G), standard molar heat

capacity (C_v) and standard molar thermal entropy (S) as well as zero-point energy (ZPE) of all the compounds are evaluated and tabulated in Table 4. All these values are obtained at 298.15 K, 1.00 atm. and calculated in units of kcal mol^{-1} (kcal mol^{-1} K^{-1} for S and C_v).

Density

Generally, high density results in higher performance.[18,42] For example, D of an explosive is proportional to its ρ, and P is proportional to the square of its ρ.[43] For an energetic material, a high value ρ means that more energy per unit volume can be packed into a volume-limited space, thereby yielding maximum violent explosion. The molecular volumes, uncorrected densities, and corrected densities are listed in Table 5. The ρ values for the designed compounds were found to be in the range from 1.91 (**E**) to 199 g cm^{-3} (**A**). Among them, compound **A** exhibited the highest density of 1.99 g cm^{-3}, which was similar to that of CL-20. Clearly, the replacement of the azo moiety with the azoxy moiety led to greater increase in density. This finding illustrated that the incorporation of highly dense groups into high-density skeletons is an effective strategy for obtaining higher density compounds. Overall, all the compounds exhibited higher

Scheme 1 Designed isodesmic reactions for the title compounds.

Table 2 Calculated total energies, zero-point energies, thermal corrections and heats of formation for the reference compounds

Comp.	E_0 (a.u.)	ZPE (kcal mol^{-1})	H_T (kJ mol^{-1})	$\Delta_f H$ (gas) (kJ mol^{-1})
CH$_4$	−40.38	28.11	10.01	−74.62
CH$_3$NO$_2$	−244.49	31.28	13.91	−81.00
A-1	−633.07	70.77	25.89	783.79
B-1	−633.07	71.17	24.68	691.53
C-1	−665.07	55.08	25.39	993.75
D-1	−665.14	56.25	25.01	834.95

Table 3 Calculated total energies (E_0), zero-point energies (ZPE), thermal corrections (H_T), gas-phase heats of formation ($\Delta H_{f,gas}$), heats of sublimation (ΔH_{sub}), and solid-phase heats of formation ($\Delta H_{f,solid}$) for the title compounds

Comp.	$\Delta H_{f,gas}{}^a$ (kJ mol^{-1})	$\Delta H_{sub}{}^b$ (kJ mol^{-1})	$\Delta H_{f,solid}{}^c$ (kJ mol^{-1})	E_0 (a.u.)	ZPE (kcal mol^{-1})	H_T (kJ mol^{-1})
A	813.85	135.79	678.06	−1449.74	76.39	53.69
B	721.59	137.86	583.73	−1449.77	76.14	53.65
C	1023.81	107.31	916.5	−1073.25	58.28	38.37
D	865.01	111.20	753.81	−1073.54	58.96	38.31
E	1172.43	79.63	1092.8	−697.09	40.34	23.64

^{a} Calculated gas-phase heat of formation. ^{b} Heat of sublimation. ^{c} Calculated solid-phase heat of formation.

calculated densities of >1.9 g cm^{-3} due to the presence of the N→O moiety, indicating that these compounds have potential as new HEDMs.

Oxygen balance and detonation performance

Oxygen balance, which indicates the degree to which an explosive can be oxidized, is an important index for identifying the potential of energetic materials as explosives or oxidants. Positive OBs indicate that there is sufficient oxygen to convert all the carbon to carbon monoxide and all the hydrogen to water, whereas negative values indicate that the oxygen content is insufficient for complete oxidation. However, too much oxygen is not favorable for improving the explosive performance of energetic compounds as additional oxygen will produce O_2, which consumes a considerable amount of energy during the explosion of energetic materials. Thus, the ideal OB value is equal to zero. All the compounds exhibited OB values between −13.68 and −26.65% mainly due to their relatively high carbon contents. By comparison, the incorporation of more –NO$_2$ groups into a molecule substantially improves its $\Delta H_{f,solid}$ and OB, eventually resulting in higher exothermicities for combustion and detonation processes.

Detonation velocity and pressure are two important performance parameters for an energetic material. Based on the calculated $\Delta H_{f,solid}$ and ρ, the detonation properties of A–E were determined using the EXPLO5 (v 6.01) program,[28] as summarized in Table 6 together with a comparison with common explosives. As shown in Table 6, the calculated D values were in the range of 9616–9943 m s^{-1}, and they were remarkably higher than those of RDX (8983 m s^{-1}) and HMX (9221 m s^{-1}). Among the compounds, E exhibited the highest D (9943 m s^{-1}), which exceeded that of CL-20 (9673 m s^{-1}). In terms of P, the P values of the designed compounds were in the range from 41.1 (D) to

44.2 GPa (C). The highest P value (C, 44.2 GPa) was much larger than those of RDX (34.9 GPa) and HMX (39.6 GPa). Overall, the detonation properties of A–E were accordingly predicted to be second only to that of CL-20, and these compounds might be the most powerful energetic materials among the CHNO-containing organic compounds.

Stability

The sensitivity of an energetic material generally refers to its vulnerability to accidental explosion caused by unintended stimuli, and it is directly related to the handling safety as well as potential application.[45] The impact sensitivity, as the most commonly used method for assessing the sensitivities of explosives, is measured by the drop height, $h_{50\%}$, where the shorter the drop height, the greater the impact sensitivity. It has been found that impact sensitivity has several strong correlations with various molecular properties.[19,46] Using four empirical models based on the properties of electrostatic potential and heat of detonation, as proposed by Rice and Hare,[31] the $h_{50\%}$ values were estimated, and the results are summarized in Table 7. Methods 1–3 showed relatively consistent results, whereas method 4 overestimated the impact sensitivities derived from the hybrid balance parameter and detonation heat. The $h_{50\%}$ values of compounds A and B were even close to that of CL-20, indicating that these two compounds are very sensitive and can be easily triggered by external stimuli such as impact. This may be because these molecules contain four strong electron-withdrawing groups, –NO$_2$, thereby reducing their stabilities to a certain extent. Compounds C–E exhibited relatively acceptable impact sensitivities with the $h_{50\%}$ values of about 30 cm, which were comparable with those of RDX (26 cm) and HMX (32 cm). Because of the complexity of the impact

Table 4 Thermochemical parameters of compounds A–E

Comp.	ZPE (kcal mol^{-1})	U (kcal mol^{-1})	H (kcal mol^{-1})	G (kcal mol^{-1})	S (kcal mol^{-1} K^{-1})	C_v (kcal mol^{-1} K^{-1})
A	76.39307	88.63139	88.632	44.12901	151.250	69.073
B	76.14081	88.37098	88.371	44.27334	149.891	69.218
C	58.27623	66.85492	66.855	31.69867	119.900	49.940
D	58.96021	67.5251	67.525	31.45206	122.978	49.389
E	40.34325	45.40098	45.401	19.10517	90.184	30.818

Table 5 Molecular volume and density for five energetic molecules

Comp.	M_w (g mol^{-1})	Volume (cm^3 mol^{-1})	$\rho_{uncorrected}$ (g cm^{-3})	$\rho_{corrected}$ (g cm^{-3})
A	356.13	178.96	2.01	1.99
B	356.13	180.23	1.98	1.97
C	268.11	137.49	1.96	1.95
D	268.11	138.20	1.95	1.94
E	180.09	95.29	1.93	1.91

Table 6 Predicted nitrogen content, oxygen balance, detonation velocity, detonation pressure, heat of detonation and explosion temperature for the title compounds

Comp.	N[a] (%)	OB[b] (%)	D[c] (m s^{-1})	P[d] (GPa)	Q[e] (kJ kg^{-1})	T_{det}[f] (K)
A	39.33	−13.48	9780	44.1	6335	4785
B	39.33	−13.48	9614	42.2	6082	4656
C	52.24	−17.90	9858	44.2	6553	4982
D	52.24	−17.90	9616	41.1	6007	4631
E	77.78	−26.65	9543	40.7	6920	5223
RDX[15]	37.84	−21.26	8983	38.0	6190	4232
HMX[15]	37.84	−21.26	9221	41.5	6185	4185
CL-20 (ref. 44)	38.36	−10.96	9673	44.9	6130	—

[a] Nitrogen content. [b] Oxygen balance for $C_aH_bO_cN_d$: $1600 \times (c - a - b/2)/M_w$, where M_w = molecular weight. [c] Detonation velocity. [d] Detonation pressure. [e] Heat of detonation. [f] Explosion temperature.

sensitivity, these estimates should be regarded as suggestive rather than conclusive results.

BDEs can provide useful information for understanding the stability of a molecule.[29] Generally, smaller BDE corresponds to a weaker bond, which makes it easier for the bond to function as a trigger bond. To investigate the thermal stabilities of the compounds of interest, the C–NO$_2$ bond was considered to be the weakest bond.[36,37] In general, if BDE > 80 kJ mol^{-1}, then the compound can be considered as a practical energetic material; otherwise, if BDE > 120 kJ mol^{-1}, then it can be considered as an excellent energetic material, which meets the stability requirements of HEDMs. Compared with TNT (251.16 kJ mol^{-1}), RDX (160.09 kJ mol^{-1}) and TATB (305.79 kJ mol^{-1}), all the designed compounds possess high BDEs and fulfill the requirements of HEDMs.[47] Furthermore, by comparing the BDEs of the title compounds, it is observed that the number of nitro groups and substituted positions have strong influence on the BDEs. The computed Wiberg bond order values, $-Q_{NO_2}$ values, and trigger lengths of the molecules are summarized in Table 7. The higher the negative charge of the nitro group, the weaker its electron-

Table 7 Calculated bond dissociation energy (BDE), Mulliken nitro group charge ($-Q_{NO_2}$), impact sensitivity ($h_{50\%}$) and electric spark sensitivity (E_{ES}) of the title compounds

Comp.	Bond	Wiberg bond order	BDE (kJ mol^{-1})	$-Q_{NO_2}$ (e)	$h_{50\%}$[a] (cm)	$h_{50\%}$[b] (cm)	$h_{50\%}$[c] (cm)	$h_{50\%}$[d] (cm)	Exp.	E_{ES} (J)
A	C1–NO$_2$	1.075	264.68	0.19	19	29	30	5	—	2.9
	C2–NO$_2$	1.040	236.85	0.22						2.5
	C9–NO$_2$	1.039	223.91	0.22						3.1
	C10–NO$_2$	1.060	254.76	0.14						3.2
B	C1–NO$_2$	1.066	270.58	0.26	21	29	32	5	—	6.3
	C3–NO$_2$	1.061	266.82	0.26						5.4
	C8–NO$_2$	1.040	223.91	0.29						4.5
	C10–NO$_2$	1.067	271.32	0.24						5.1
C	C1–NO$_2$	1.077	257.33	0.25	42	30	34	7	—	8.6
	C10–NO$_2$	1.070	255.22	0.23						9.2
D	C2–NO$_2$	1.0488	264.68	0.25	58	30	36	7	—	10.2
	C9–NO$_2$	1.040	263.89	0.24						9.4
E	—	—	—	—	88	30	45	9	—	—
RDX					49	31	39	22	28	—
HMX					21	31	41	22	32	—
CL-20					16	29	29	3	14	—

[a] Method 1 is related to the GIPF parameters $|\bar{V}^+ - |\bar{V}^-||$. [b] Method 2 is related to the GIPF balance parameter ν. [c] Method 3 is related to the heat of detonation Q. [d] Method 4 is related to the hybrid model using Q and ν.

withdrawing ability and the greater the overall stability of the compound, which lowers its impact sensitivity. Wiberg bond order values also reflect the strength of a trigger bond, where a large Wiberg bond order value indicates that the bond is difficult to rupture and thus, the molecule is stable. The calculated $-Q_{NO_2}$ values vary from 0.14 to 0.29 eV, and they are found to be higher than those of CL-20 (0.08 eV), HMX (0.11 eV) and RDX (0.13 eV),[48] suggesting that these compounds have very low sensitivity.

Potential HEDM candidates

It is well-known that a good nitrogen-rich HEDM candidate should have not only excellent detonation properties but also good stability. Fig. 7 presents the detonation velocity and pressure, density and impact sensitivity used to evaluate the overall performance of the azoxy-fused tricyclic compounds compared with those of RDX, HMX and CL-20. As far as we know, the challenges in the development of HEDMs include the search for materials with higher performance, better safety, and improved environmental compatibility. However, in most cases, stability decreases as the energy increases. It can be shown that all azoxy-fused tricyclic compounds show relatively high densities and detonation properties when compared with commonly used explosives such as RDX, HMX and CL-20.

This is mainly because these compounds have very high positive $\Delta H_{f,solid}$ as nitrogen-rich molecules. Among all the designed compounds, **A** has the highest ρ value (1.99 g cm^{-3}), whereas it has the lowest $h_{50\%}$ value, which limits its application in the future. For compound **E**, although it has good stability, its energetic properties (*P*: 40.7 GPa and *D*: 9543 m s^{-1}) are disadvantageous compared to those of the other four compounds. Fortunately, it is surprising that

compounds **B–D** perform better than HMX similar to CL-20, which results in relative balance between detonation properties and stability. Therefore, **B–D** may be considered as potential HEDM candidates with improved stability and performance.

Conclusion

In summary, we systematically investigated the molecular structures, electronic structures, heats of formation, energetic properties, and thermal stabilities of five novel azoxy non-hydrogen-containing 5/6/5 fused tricyclic compounds. Their optimized molecular geometries showed that two five-membered azole heterocycles are fused to 1,2,3,4-tetrazine with a common C–N bond. In addition, the three heterocycles in the fused tricyclic system and the N→O bond were coplanar, whereas the nitro groups deviated from the ring plane, implying that their electronic properties play an important role in their molecular structures. Additionally, the surface minima and maxima of ESP displayed a visual representation of their chemically active sites. The theoretical IR spectra data were simulated to confirm the identification of the target compounds. The effects of different skeleton structures on the density, heat of formation, denotation velocity and pressure well as stability of the novel azoxy non-hydrogen-containing 5/6/5 fused tricyclic compounds were also investigated. When the length of the catenated nitrogen chain was elongated in their molecular structures, the heat of formation increased. Among these compounds, compound **E** exhibited the highest heat of formation of 1092.8 kJ mol^{-1}, and **A** exhibited the highest density of 1.99 g cm^{-3}.

The critical energetic properties and stabilities of all the compounds have been estimated. Their densities range from 1.91 to 1.99 g cm^{-3}. Compared with the azo non-hydrogen-containing 5/6/5 fused compounds, the compounds containing the azoxy moiety can enhance density effectively. However, the azoxy moiety is not beneficial for obtaining energetic molecules with high positive heat of formation in this system, which indicates that the azoxy moiety has both positive and negative effects on their properties, *i.e.*, high densities are obtained, but the heats of formation are low. All the compounds show higher detonation velocities (9543-9858 m s^{-1}) and pressures (40.7–44.1 GPa). By comprehensive analysis, we infer that compounds **B–D** perform better than HMX similar to CL-20, which results in a relative balance between detonation properties and stability. Therefore, compounds **B–D** may be considered as potential HEDM candidates with improved stability and performance. In addition, our design strategy, involving the combination of the azoxy moiety and fused tricyclic skeleton for the construction of nitrogen-rich molecular structures with high density and positive HOFs, is a valuable approach for the development of novel HEDMs with excellent performance and stability.
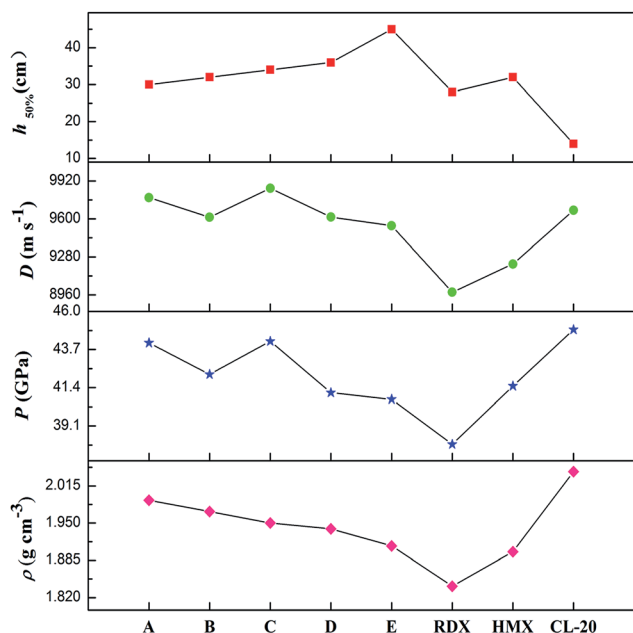

Fig. 7 Overall performances of the azoxy-fused tricyclic compounds compared with those of RDX, HMX and CL-20.

Conflicts of interest

There are no conflicts to declare.

Acknowledgements

Notes and references

1 T. G. Witkowski, E. Sebastiao, B. Gabidullin, A. Hu, F. Zhang and M. Murugesu, *ACS Appl. Energy Mater.*, 2018, **1**, 589–593.

2 D. E. Chavez, S. K. Hanson, J. M. Veauthier and D. A. Parrish, *Angew. Chem., Int. Ed.*, 2013, **52**, 6876–6879.

3 C. L. He, H. X. Gao, G. H. Imler, D. A. Parrish and J. M. Shreeve, *J. Mater. Chem. A*, 2018, **6**, 9391–9396.

4 T. M. Klapötke, P. C. Schmid, S. Schnell and J. Stierstorfer, *Chem.–Eur. J*, 2015, **21**, 9219–9228.

5 M. S. Klenov, A. A. Guskov, O. V. Anikin, A. M. Churakov, Y. A. Strelenko, I. V. Fedyanin, K. A. Lyssenko and V. A. Tartakovsky, *Angew. Chem., Int. Ed.*, 2016, **55**, 11472–11475.

6 D. G. Piercey, D. E. Chavez, B. L. Scott, G. H. Imler and D. A. Parrish, *Angew. Chem., Int. Ed.*, 2016, **55**, 15315–15318.

7 T. M. Klapötke, P. C. Schmid, S. Simon and J. Stierstorfer, *Chem.–Eur. J.*, 2015, **21**, 9219–9228.

8 D. E. Chavez, J. C. Bottaro, M. Petrie and D. A. Parrish, *Angew. Chem., Int. Ed.*, 2015, **54**, 12973–12975.

9 Y. Tang, D. Kumar and J. M. Shreeve, *J. Am. Chem. Soc.*, 2017, **139**, 13684–13687.

10 P. Yin, J. Zhang, G. H. Imler, D. A. Parrish and J. M. Shreeve, *Angew. Chem., Int. Ed.*, 2017, **56**, 8834–8838.

11 Y. Qu and S. P. Babailov, *J. Mater. Chem. A*, 2018, **6**, 1915–1940.

12 Y. Li, C. Qi, S. Li, H. Zhang, C. Sun, Y. Yu and S. Pang, *J. Am. Chem. Soc.*, 2010, **132**, 12172–12173.

13 T. M. Klapötke and D. G. Piercey, *Inorg. Chem.*, 2011, **50**, 2732–2734.

14 F. Boneberg, A. Kirchner, T. M. Klapötke, D. G. Piercey, M. J. Poller and J. Stierstorfer, *Chem.–Asian J.*, 2013, **8**, 148–159.

15 D. Fischer, T. M. Klapötke, D. G. Piercey and J. Stierstorfer, *Chem.–Eur. J.*, 2013, **19**, 4602–4613.

16 A. A. Dippold, D. Izsák and T. M. Klapötke, *Chem.–Eur. J.*, 2013, **19**, 12042–12051.

17 J. Zhang and J. M. Shreeve, *J. Phys. Chem. C*, 2015, **119**, 12887–12895.

18 M. A. Kettner, K. Karaghiosoff, T. M. Klapötke, M. Sućeska and S. Wunder, *Chem.–Eur. J.*, 2014, **20**, 7622–7631.

19 J. Zhang and J. M. Shreeve, *J. Am. Chem. Soc.*, 2014, **136**, 4437–4445.

20 M. J. Frisch, G. W. Trucks, H. B. Schlegel, G. E. Scuseria, M. A. Robb, J. R. Cheeseman, G. Scalmani, V. Barone, B. Mennucci, G. A. Peterssonand *et al.*, *Gaussian 09, Revision A.1*, Gaussian, Inc., Wallingford, CT, 2009.

21 P. W. Atkins, *Physical Chemistry*, Oxford University Press, Oxford, U.K., 1982.

22 P. Politzer and J. S. Murray, *Cent. Eur. J. Energ. Mater.*, 2011, **8**, 209–220.

23 P. Politzer, P. Lane and J. S. Murray, *Cent. Eur. J. Energ. Mater.*, 2011, **8**, 39–52.

24 E. F. C. Byrd and B. M. Rice, *J. Phys. Chem. A*, 2006, **110**, 1005–1013.

25 M. Jaidann, S. Roy, H. Abou-Rachid and L. Lussier, *J. Hazard. Mater.*, 2010, **176**, 165–173.

26 F. Wang, H. Du, J. Zhang and X. Gong, *J. Phys. Chem. A*, 2011, **115**, 11852–11860.

27 T. Lu and F. Chen, *J. Comput. Chem.*, 2012, **33**, 580–592.

28 M. Sućeska, *EXPLO5, version 6.01*, Brodarski Institute, Zagreb, Croatia, 2013.

29 S. J. Blanksby and G. B. Ellison, *Acc. Chem. Res.*, 2003, **36**, 255–263.

30 P. He, J. Zhang, L. Wu, J. Wu and T. Zhang, *J. Phys. Org. Chem.*, 2017, **30**, e3674.

31 B. M. Rice and J. J. Hare, *J. Phys. Chem. A*, 2002, **106**, 1770–1783.

32 Q. Zhang, J. Zhang, X. Qi and J. M. Shreeve, *J. Phys. Chem. A*, 2014, **118**, 10857–10865.

33 Z. Chunyan, C. Xinlu and Z. Feng, *Propellants, Explos., Pyrotech.*, 2010, **35**, 555–560.

34 P. Yin and J. M. Shreeve, *Angew. Chem., Int. Ed.*, 2015, **54**, 14513–14517.

35 J. S. Murray and P. Politzer, *Wiley Interdiscip. Rev.: Comput. Mol. Sci.*, 2011, **1**, 153–163.

36 T. Schmalz, W. A. Seitz, D. J. Klein and G. Hite, *J. Am. Chem. Soc.*, 1988, **110**, 1113–1127.

37 Z. Zhou and R. G. Parr, *J. Am. Chem. Soc.*, 1989, **111**, 7371–7379.

38 H. Dong and F. Zhou, *High energy explosives and correlative physical properties*, Science Press, Beijing, 1989.

39 P. He, J. Zhang, K. Wang, X. Yin, X. Jin and T. Zhang, *Phys. Chem. Chem. Phys.*, 2015, **17**, 5840–5848.

40 E. D. Glendening, C. R. Landis and F. Weinhold, *Wiley Interdiscip. Rev.: Comput. Mol. Sci.*, 2012, **2**, 1–42.

41 T. Zhang, L. Liu, C. Li, Y. Zhang, Z. Li and S. Zhang, *J. Mol. Struct.*, 2014, **1067**, 195–204.

42 T. Fei, Y. Du and S. Pang, *RSC Adv.*, 2018, **8**, 10215–10227.

43 J. Zhang, H. Su, Y. Dong, P. Zhang, Y. Du, S. Li, M. Gozin and S. Pang, *Inorg. Chem.*, 2017, **56**, 10281–10289.

44 D. Fischer, J. L. Gottfried, T. M. Klapötke, K. Karaghiosoff, J. Stierstorfer and T. G. Witkowski, *Angew. Chem., Int. Ed.*, 2016, **55**, 16132–16135.

45 A. K. Sikder and N. Sikder, *J. Hazard. Mater.*, 2004, **112**, 1–15.

46 F. A. Bulat, A. Toro-Labbé, T. Brinck, J. S. Murray and P. Politzer, *J. Mol. Model.*, 2010, **16**, 1679–1691.

47 Q. Ma, T. Jiang, X. Zhang, G. Fan, J. Wang and J. Huang, *J. Phys. Org. Chem.*, 2015, **28**, 31–39.

48 Y. Shu, H. Li, S. Gao and Y. Xiong, *J. Mol. Model.*, 2013, **19**, 1583–1590.